Journal of Hydrology 519 (2014) 1506–1515

Contents lists available at ScienceDirect

Journal of Hydrology

journal homepage: www.elsevier.com/locate/jhydrol

A conservative flow routing formulation: Déjà vu and the variable-parameter Muskingum method revisited

Paolo Reggiani [a,b,*], Ezio Todini [c], Dennis Meißner [d]

[a] Research Institute for Water and Environment, Department of Civil Engineering, University of Siegen, 57068 Siegen, Germany
[b] Deltares, P.O. Box 177, 2600MH Delft, The Netherlands
[c] Department of Biological, Geological and Environmental Sciences, University of Bologna, Via Zamboni 67, 40126 Bologna, Italy
[d] Bundesanstalt für Gewässerkunde, Am Mainzer Tor 1, 56068 Koblenz, Germany

ARTICLE INFO

Article history:
Received 26 November 2013
Received in revised form 7 June 2014
Accepted 29 August 2014
Available online 16 September 2014
This manuscript was handled by Andras Bardossy, Editor-in-Chief

Keywords:
Channel routing
Variable-parameter Muskingum
Finite-dimension formulation
Flux closure
Mass and momentum conservation

SUMMARY

A wide range of approaches are used for flow routing in hydrological models. One of the most attractive solutions is the variable-parameter Muskingum (VPM) method. Its major advantage consists in the fact that *(i)* it can be applied to poorly-gauged basins with unknown channel geometries, *(ii)* it requires short execution time and *(iii)* it adequately captures, also in the presence of mild slopes, the most salient features of a dynamic wave such as the looped rating curve and the steepening of the rising limb of the hydrograph. In addition, the method offers the possibility to derive average water levels for a reach segment, a quantity which is essential in flood forecasting and flood risk assessment. For reasons of computational economy the method is also appropriate for applications, in which hydrological and global circulation models (GCM) are coupled, and where computational effort becomes an issue. The VPM approach is presented from a philosophical and conceptual perspective, by showing the derivation of its mass and momentum balance properties from the point to the finite scale, and by demonstrating its strengths by means of an application in an operational context. The principal novel contributions of the article relate to *(a)* the extension of the Muskingum–Cunge–Todini approach to accept uniformly distributed lateral inflow, *(b)* the use of power law cross sections and *(c)* the validation of the method through a long-term simulation of a real-world case, including the comparison of results to those obtained using a full Saint Venant equations model.

1. Introduction

The spectrum of channel routing methods in hydrological applications is broad. The options reach from simple linear translation models to a complete dynamic description of channel flow at the other end. The choice usually depends on the scientific background of the modeller and the particular problem at hand. Hydrologist generally opt for conceptual approaches, while people with a channel hydraulics background prefer physically-based solutions, starting out from the full dynamic wave model or simplifications thereof. Examples include the simplification of the dynamic wave model to obtain a hyperbolic differential equation (Price, 1985), or the diffusion wave (DW) analogy formulated as parabolic equation by combining mass and momentum conservation, while neglecting acceleration terms (Hayami, 1951; Lighthill and Whitham, 1955; Dooge, 1973). The DW can be used as linear model with constant parameters for which an integral analytical solution can be found (Hayami, 1951; Dooge, 1973), or as a linear model with variable parameter values locally linearised in time as in Todini and Bossi (1986). The non-linear version with variable parameters is more complex and needs to be solved numerically. Examples include the work by Cappelaere (1997) and the recent note by Price (2009).

A further simplification of the full dynamic model is the kinematic wave, in which the friction slope is assumed equal to the bed slope. This is possible when the kinetic and the inertial gradients are negligible with respect to the bed and friction slopes. In analogy to the DW, the kinematic model can be formulated with constant or variable parameters, obtaining a linear or non-linear version respectively. The integral form of the kinematic model leads to a linear (Nash, 1957; Ostrowski, 1992) or non-linear (Liu and Todini, 2004) reservoir equation, for which analytical solutions can be found. However, while reservoir cascades may be appropriate for flow routing within well defined application limits, a more complete dynamic routing becomes indispensable when

* Corresponding author at: Research Institute for Water and Environment, Department of Civil Engineering, University of Siegen, 57068 Siegen, Germany.

http://dx.doi.org/10.1016/j.jhydrol.2014.08.057
0022-1694/

describing channel flow of large systems also in presence of very mild slopes (in the order of 10^{-4}), where the kinetic and inertial gradients become relevant.

In this context Gąsiorowski and Szymkiewicz (2007) have provided a significant contribution towards the understanding of conservation properties of the non-linear kinematic and DW equations. Their analysis of integral terms demonstrates that by integrating variable-parameter models, whose governing equations hold at the point-scale, over finite time and space domains, mass and momentum cannot be simultaneously conserved while only linear (thus constant-parameter) models remain conservative in the finite-dimension form. The reason is the non-divergent form of the non-linear governing equation. These considerations are interesting, because the conservation properties of widely used models have rarely been addressed from a purely analytical perspective and hardly has any attention ever been paid to the conservation of momentum. Said conservation properties require an a priori knowledge on the operational limits of a particular model and for this reason form a central topic of this paper.

A commonly used alternative to the dynamic wave model is the variable-parameter Muskingum (VPM) routing method. Cunge (1969) modified the original fixed-parameter linear approach introduced by McCarthy (1940), which he interpreted as a first-order kinematic approximation of a DW model. He changed it into a non-linear parabolic model by allowing for variable parameters. These are then defined by imposing a match between physical and numerical diffusion. Todini (2007) revised and generalised the VPM method by delivering an explanation for why the original Cunge scheme is not mass-conservative, as repeatedly observed several years earlier (Ponce and Yevjevich, 1978; Tang et al., 1999; Cunge, 2001). The principal strength of the VPM approach remains the fact that it can be implemented with comparatively modest input data and does not require detailed channel geometries. The latter are needed by the full dynamic wave model, but are frequently unavailable in practice. Moreover the computational demand is comparatively low, making the approach appealing for representing surface flows in complex land-surface schemes within global circulation model (GCM) simulations.

Aim of this paper is to take a fresh look at the VPM method, especially the mass-conservative formulation (MCT) introduced by Todini (2007), by casting it in the light of a conservative finite-dimension formulation and integrating the point-scale conservation equations for mass and momentum over a channel reach segment.

In addition to showing the conservation properties of MCT, the principal novel aspects of the paper are: *(1)* the extension of the MCT method to accept uniformly distributed lateral inflow; *(2)* the use of power law cross sections, which can be related to the physographic characteristics of catchments (Leopold and Maddock, 1953); and *(3)* the application of MCT to a dendritic channel network for long-term (i.e. 6 years) simulations in a real-world case, as opposed to its application over a straight channel (Todini, 2007), and the comparison of results with those obtained using a complete Saint–Venant model.

The paper is structured as follows: Section 2 provides an overview of integration of the mass and momentum conservation equations from the point to the channel reach scale, Section 3 sets the Muskingum method into perspective as an finite-dimension approach, Sections 4 and 5 describe an application to a real world case, Section 6 presents the results, while Section 7 is dedicated to a discussion over the VPM method.

2. Mass and momentum conservation across scales

In following paragraphs we show how mass and momentum can only be conserved by scaling, through integration, the conservation equations from the microscale to the finite scale of a channel reach. The entire integration path is presented, to demonstrate how the Saint–Venant equations can be viewed as an intermediate step between a micro-scale and a finite-dimension formulation. On the contrary, the Muskingum method, which is central to this paper, is a finite-dimension formulation. To derive the Muskingum formulation by starting all the way from the micro-scale, allows one to analyse its conservative properties and to show its relation to infinitesimal-scale formulations, such as the DW and Saint–Venant model, and their discrete solutions.

2.1. Microscale formulation

The conservation equations for a generic hydrodynamic property $\rho\psi$ (e.g. mass, momentum or energy) of a fluid at the microscale can be written in tensor notation as follows (Eringen, 1980):

$$\frac{\partial(\rho\psi)}{\partial t} + \nabla\cdot(\rho\psi\mathbf{v}) - \nabla\cdot\mathbf{i} - \rho f = 0 \tag{1}$$

where $\mathbf{i}$ is a diffusive flux and f is an external supply of ψ. To obtain microscale mass, momentum and energy equations, $\psi, \mathbf{i}$, and f are replaced by the properties listed in Table 1, where $\mathbf{t} = -p\mathbf{I} + \boldsymbol{\tau}$ is the total stress tensor, p the pressure, $\mathbf{I}$ the identity matrix and $\boldsymbol{\tau}$ the viscous stress tensor. For an incompressible fluid the microscale mass and momentum equations become:

$$\nabla\cdot\mathbf{v} = 0 \tag{2}$$

and

$$\rho\frac{\partial\mathbf{v}}{\partial t} + \rho\nabla\cdot(\mathbf{v}\,\mathbf{v}) - \nabla\cdot\mathbf{t} - \rho\,\mathbf{g} = 0 \tag{3}$$

respectively, whereby ψ is set equal to the velocity $\mathbf{v}$, $\mathbf{i}$ to the total stress tensor $\mathbf{t}$ and f to the gravity vector $\mathbf{g}$. The mechanical energy conservation is obtained by setting ψ equal to the kinetic energy per unit mass, $v^2/2$, $\mathbf{i}$ to the rate of work by internal stresses, $\mathbf{t}\cdot\mathbf{v}$, and f to the rate of work by gravity, $\mathbf{g}\cdot\mathbf{v}$. The latter is listed for sake of completeness and will not be used further.

2.2. Infinitesimal-scale formulation

The dynamic wave model, known as Saint–Venant (SV) equations, is derived by averaging the microscale Eqs. (2) and (3) over a slab of infinitesimal thickness orthogonal to the channel axis. In the averaging process the SV assumptions (Chow, 1968) are applied. The resulting 1-D mass conservation equation, which is now infinitesimal along the channel axis and finite-dimension over the cross-section, becomes:

$$\frac{\partial A}{\partial t} + \frac{\partial Q}{\partial x} = 0 \tag{4}$$

with Q the discharge and A the cross-section area at axis point x and time t. Similarly the infinitesimal momentum equation averaged over the slab reads:

$$\frac{\partial Q}{\partial t} + \frac{\partial\left(Q^2/A\right)}{\partial x} + gA\left(\frac{\partial y}{\partial x} - S_0\right) + gAS_f = 0 \tag{5}$$

where y is the flow depth, S_0 is the local bed slope and S_f the friction slope. S_f can be related via Manning law to the steady-state

Table 1
Summary of the property ψ expressions in the microscale conservation equation.

Property	ψ	$\mathbf{i}$	f
Mass	1	0	0
Momentum	$\mathbf{v}$	$\mathbf{t}$	$\mathbf{g}$
Mechanical energy	$v^2/2$	$\mathbf{t}\cdot\mathbf{v}$	$\mathbf{g}\cdot\mathbf{v}$

discharge Q_0 and the local hydraulic radius. After rearranging corresponding terms, the following expression is obtained:

$$Q = Q_0\left[1 - \frac{1}{S_0}\frac{\partial y}{\partial x} - \frac{1}{S_0 gA}\frac{\partial\left(Q^2/A\right)}{\partial x} - \frac{1}{S_0 gA}\frac{\partial Q}{\partial t}\right]^{1/2} \tag{6}$$

Eq. (6) highlights which terms contribute to the local discharge under dynamic conditions by adding correction terms to Q_0. Depending on a particular situation, individual terms between square brackets have higher importance over others, which become negligible. For instance in the case of a kinematic wave, the surface gradient, as well as the convective and local acceleration become unimportant (Moussa and Bocquillon, 1996; Moramarco et al., 2008). In the diffusive wave model the two acceleration terms can be dropped, while the full dynamic wave model requires all acceleration components to be retained. The set of Eqs. (4) and (5) constitutes the dynamic wave model and needs to be solved numerically. Under assumption of negligible inertia and linearisation (Hayami, 1951; Lighthill and Whitham, 1955; Dooge, 1973) or by applying perturbation analysis (Price, 1985), (4) and (5) can be merged first into a hyperbolic and then a parabolic infinitesimal-scale equation (infinitesimal along the channel axis and finite-dimensional over the cross-section) in only Q (or alternatively y), known as diffusive wave (DW) model:

$$\frac{\partial Q}{\partial t} + C(y, \partial y/\partial x)\,\frac{\partial Q}{\partial x} + D(y, \partial y/\partial x)\,\frac{\partial^2 Q}{\partial x^2} = 0 \tag{7}$$

with C the celerity and D the diffusion coefficient, which expresses the wave attenuation, both non-linear functions of y and $\partial y/\partial x$, also replaceable by Q and $\partial Q/\partial x$ (Cappelaere, 1997). For constant parameters a linear DW is obtained, for which analytical solutions were found by Hayami (1951) through perturbation analysis or by Dooge (1973) on the basis of Laplace transforms. Todini and Bossi (1986) proposed a solution for the locally linearised DW equation with stepwise constant parameters.

The infinitesimal-scale equation has unfortunately been frequently "stretched" over a finite dimension by numerically integrating it in time and space using the Finite Difference approach. There are two main reasons for avoiding this approach: firstly, as pointed out by Gąsiorowski and Szymkiewicz (2007), Eq. (7) with variable parameters cannot be written in divergent form, as it has been obtained on the basis of simplifying assumptions, among which the zero-inertia hypothesis. Secondly, by "stretching" the infinitesimal solution as to represent the average spatial behaviour between adjacent grid cells, one implicitly assumes that the infinitesimal equations, as well as the domain characteristics and their parameters values, are uniform at each point of the spatial integration domain, so that one can state:

$$f\left(\overline{y}, \overline{Q}|\overline{\boldsymbol{\theta}}\right) \cong \overline{f}_L = \frac{1}{L}\int_L f[y(x,t), Q(x,t)|\boldsymbol{\theta}(x,t)]dx \tag{8}$$

where $f(\,)$ represents the partial differential equation, $\boldsymbol{\theta}(\,)$ the domain characteristics vector including the parameter values, L the distance between grid centre points, and $^-$, the expected value operator. Unfortunately this is not the case due to the large spatial variability of cross sections and roughness properties in natural rivers, combined with the non-linearity of $f(\,)$, because the expected value of a non-linear function does not equate the function evaluated at expected values, unless all parameters and related quantities are uniform over the integration domain. As integration in time is not that critical because of the reduced size of the time integration step, finite differences can still be used in time after averaging the equations in space, which become ordinary differential equations as a consequence.

2.3. Finite-dimension formulation

In a the finite-dimension scale, Eq. (1) is averaged (integrated) over a control volume, which we define as a channel segment of finite length. Application of Reynolds transport and Gauss theorems allows converting the volume integral of spatial gradients into fluxes across the external boundary surface A of the control volume:

$$\frac{d}{dt}\int_V \rho\psi dV + \int_A \mathbf{n}\cdot[\rho(\mathbf{v}-\mathbf{w})\psi - \mathbf{i}]dA - \int_V \rho f dV = 0 \tag{9}$$

where $\mathbf{n}$ is the unit normal to A pointing outward, $\mathbf{v}$ is the fluid velocity and $\mathbf{w}$ is the velocity of the boundary surface A at a point (e.g. if the water free surface moves or the bed surface changes due to erosion/sedimentation). The finite-dimension mass and momentum balance equations are obtained by inserting the corresponding properties $\psi, \mathbf{i}$, and f according to Table (1). For constant mass density and static control volume boundaries, where $\mathbf{w} = 0$, the finite-dimension formulation of the mass and momentum balance equations reduce to

$$\frac{d}{dt}\int_V dV + \int_A \mathbf{n}\cdot\mathbf{v}dA = 0 \tag{10}$$

and to the vector equation

$$\frac{d}{dt}\int_V \rho\mathbf{v}dV + \int_A \mathbf{n}\cdot[\rho\mathbf{v}\mathbf{v} - \boldsymbol{\tau}]dA + \int_A \mathbf{n}\,pdA = \int_V \rho\mathbf{g}dV \tag{11}$$

respectively. The portion of boundary surface A crossed by mass fluxes and pressure forces are the upstream and down-stream cross sections of the reach segment, while the channel bed is affected by shear stresses. We note that (11) needs to be projected along the direction of the channel axis. In light of the analysis performed by Gąsiorowski and Szymkiewicz (2007), the microscale equations stated in conservative form, have been mapped into a finite-scale balance law via integration. No additional terms are needed to balance the sum of terms in (10). Appendix A provides the proof that the finite-dimension momentum balance law (11) is also conservative.

On the contrary, space–time integration of the infinitesimal-scale diffusive wave Eq. (7) over a finite reach segment, as when using finite difference approaches, will always lead to a non-zero residual term, which is needed to balance the rate of change and boundary flux terms of Q, with the exception of the linear case with constant parameters C and D. This is due to the fact that for variable parameters the convective and diffusive flux terms cannot be stated in divergent form, with the consequence that the finite-scale mass and momentum conservation will be inevitably affected. The proof is provided in Appendix B. The mass error in (7) depends among others on the wave slope $\partial Q/\partial x$ and may well be small for smooth waves. However, as shown on theoretical grounds, the error is structural. We conclude that the finite-dimension mass balance in the form (10) is a conceptually correct conservation law to be used as basis for a mass-conservative Muskingum flow formulation at the finite or reach scale.

3. Muskingum as finite-dimension formulation

The principal challenge in a finite-dimension formulation consists in closing boundary flux terms. These can for instance be related to independent state variables of the system. Here we focus on the finite-scale mass conservation law (10), which can be stated more concisely in terms of the flux I entering the segment through the upstream boundary, the flux O exiting at the downstream end and the lateral inflow Q^L:

$$\frac{dV}{dt} = I - O + Q^L \tag{12}$$

We note that in line with the finite-dimension formulation, the fluxes I and O are defined on the cross-section interface between two reach elements and not at the reach midpoint.

McCarthy (1940) observed that the reach segment volume can be approximated linearly as the sum of a prism and a wedge, and can thus be expressed as linear combination of I and O, where the constant k has dimension $[T]$ and ϵ is dimensionless:

$$V = \epsilon k\, I + (1-\epsilon) k\, O \tag{13}$$

from which a linear storage-flux function $O = O(I, V, Q^L)$ can be explicated. Cunge (1969) introduced variable k and ϵ, allowing for a non-linear storage-flux relationship, hence known as Muskingum–Cunge (MC) routing. As recently pointed out by Todini (2007) the derivative of (13) must in that case be obtained by considering the coefficients as functions of time, a facet that had been overlooked by Cunge (1969) and successive works (Ponce and Yevjevich, 1978; Ponce and Chaganti, 1994), but which is essential for ensuring mass conservation and consistency with the steady state. When the parameters are not constant in time, their expression cannot be taken out of the derivative operator and thus (Todini, 2007) the total derivative of storage in presence of variable parameters becomes:

$$\begin{aligned}\frac{dV}{dt} &= \frac{d[\epsilon k\, I]}{dt} - \frac{d[(1-\epsilon)kO]}{dt} \\ &= \epsilon k \frac{dI}{dt} + I\frac{d[\epsilon k]}{dt} - (1-\epsilon)k\frac{dO}{dt} - O\frac{d[(1-\epsilon)k]}{dt}\end{aligned} \tag{14}$$

By setting (12) equal to (14) and switching to a discrete notation in time, (14) can be restated:

$$\overline{\epsilon k}\,\frac{\Delta I}{\Delta t} + \frac{\Delta[\epsilon k]}{\Delta t}\,\bar{I} - \overline{(1-\epsilon)k}\,\frac{\Delta O}{\Delta t} - \frac{\Delta[(1-\epsilon)k]}{\Delta t}\,\bar{O} = \bar{I} - \bar{O} + \bar{Q}^L \tag{15}$$

where the time-average $\bar{}$, is defined as $\frac{1}{2}(|_{t+\Delta t} + |_t)$ and the difference $\Delta = |_{t+\Delta t} - |_t$. After rearranging the expression, the outgoing flux $O_{t+\Delta t}$ can be stated as non-linear combination of fluxes with variable parameters:

$$O_{t+\Delta t} = C_1\, I_{t+\Delta t} + C_2\, I_t + C_3\, O_t + C_4 \overline{Q}^L \tag{16}$$

A physical interpretation of k and ϵ has been performed first by Cunge (1969) for a segment of length Δx, width B and slope S_0, whereby he set the numerical diffusion (higher order numerical rounding error) in a finite difference mid-point scheme of the kinematic wave model equal to the coefficient of the second-order term in the DW model. Todini (2007) in his revised mass-conservative and steady-state consistent analysis redefined the original $k = \Delta x/c$ with $c\,[L/T]$ the wave celerity, as $k^* = \Delta x/v$ with $v\,[L/T]$ the reach velocity and ϵ as

$$\epsilon^* = \frac{1}{2}\left(1 - \frac{q\,v}{c^2 \Delta x B S_0}\right) \tag{17}$$

where q is a reference discharge, a quantity which can be estimated explicitly (Cunge, 1969; Ponce and Yevjevich, 1978) or implicitly at the grid nodes using multiple support points (Ponce and Chaganti, 1994). The full development of (16) is given in Appendix C.

In this paper we have introduced the possibility of lateral inflow to the MCT method. Inclusion of lateral inflow in the original constant-parameter Muskingum method was first proposed by O' Donnell (1985) via a third parameter in addition to the original parameters k and ϵ, by concentrating it at the upper and lower reach ends. Ponce (1986) reformulated the problem for the case of the VPM method and derived a fourth coefficient, as a function of the two Muskingum–Cunge parameters. Ponce never provided its mathematical derivation, but starting from the results it was possible to re-derive it. Since inclusion of lateral inflow into a model such as the Muskingum, must account for its lumped nature, Ponce (1986) reformulated the problem for the case of the VPM method (Cunge, 1969) and derived a coefficient as a function of the Courant and cell Reynolds numbers, which can be expressed in terms of the two MC parameters, namely k and ϵ. The lateral inflow in Ponce's approach is only explicitly accounted for in the mass balance equation (Eq. (12)), while it is not in the second equation (Eq. (13)), expressing the storage as a weighted average of inflow and outflow. The rationale of this approach lies in the fact that the outflow of the reach implicitly takes the effect of the lateral inflow into account. Ponce's (1986) approach was referenced in the HEC-RAS user manual (USACE, 1990) and in Ponce and Lugo (2001). In this paper the extension of the Ponce (1986) approach into the MCT (Todini, 2007) is presented. At the same time, since Ponce never provided its mathematical derivation, it was felt useful to provide the rationale and the mathematical derivation of the fourth coefficient in Appendix C. The proposed approach, which is coherent with the lumped nature of MC/MCT, is totally unrelated to the Price (2009) derivation, which is relevant for a finite difference approach.

4. Application

To verify the MCT for a real-world case it was applied to flood propagation in the river Mosel. The Mosel drains a 29,000 km^2 basin, and is one of the largest tributaries of the river Rhine (Fig. 1a). The annual flow at Koblenz is about 330 m^3/s. The hydrological outflow section of the basin is considered at gauging station Cochem, about 50 km upstream from Koblenz. Peak discharges of approximately 4200 m^3/s have been recorded, making the Mosel a significant flow contributor to the Rhine. Accurate flow forecasting on the river Mosel is important, and attracts stakeholder interest to compare computational and forecasting performance of non-linear routing methods. A drawback of using the Mosel river system for the present study is the high level of river training, as the Mosel also serves navigation and hydro-electric generation purposes. The engineering works have a severe impact on low flow regimes, but their effect is felt more during low flow periods and gradually disappears during medium to high flows, where the structures are operated in such a way as to allow floods to propagate undisturbed.

5. Simulations

The verification is performed on hand of flow simulations for the 1/1/1996–31/12/2001 period. The lateral inflows were generated using raw forcing data on the REW hydrological model (Reggiani and Rientjes, 2005, 2010). No data assimilation or input correction was applied to the hydrological model with the aim to address input uncertainty. As a result the reproduction of observed flow is not optimal. However, main purpose of this exercise is to compare the MCT performance against the dynamic wave solver SOBEK (Stelling and Verwey, 2005), which is used for flow forecasting operations by the Federal Institute of Hydrology (BfG), and serves as reference case. The channel geometry for the MCT, mainly the top width B and celerity $c = \partial Q/\partial A$ are determined on the basis of a combination of the at-a-station and downstream hydraulic geometry relationships by Leopold and Maddock (1953), as described in Snell and Sivapalan (1995) and also used by Reggiani et al. (2014) on the River Mosel. The reach segments have been set to a length of 1 km.

In SOBEK 455 surveyed high-resolution cross sections were used, about one every 500 m. The computational grid includes 726 nodes over a total model length of 240 km. The Manning roughness is variable with values ranging between 0.022 and 0.025. Fig. 1b shows a schematic view of the model setup. The upper boundary conditions for SOBEK are imposed as flow

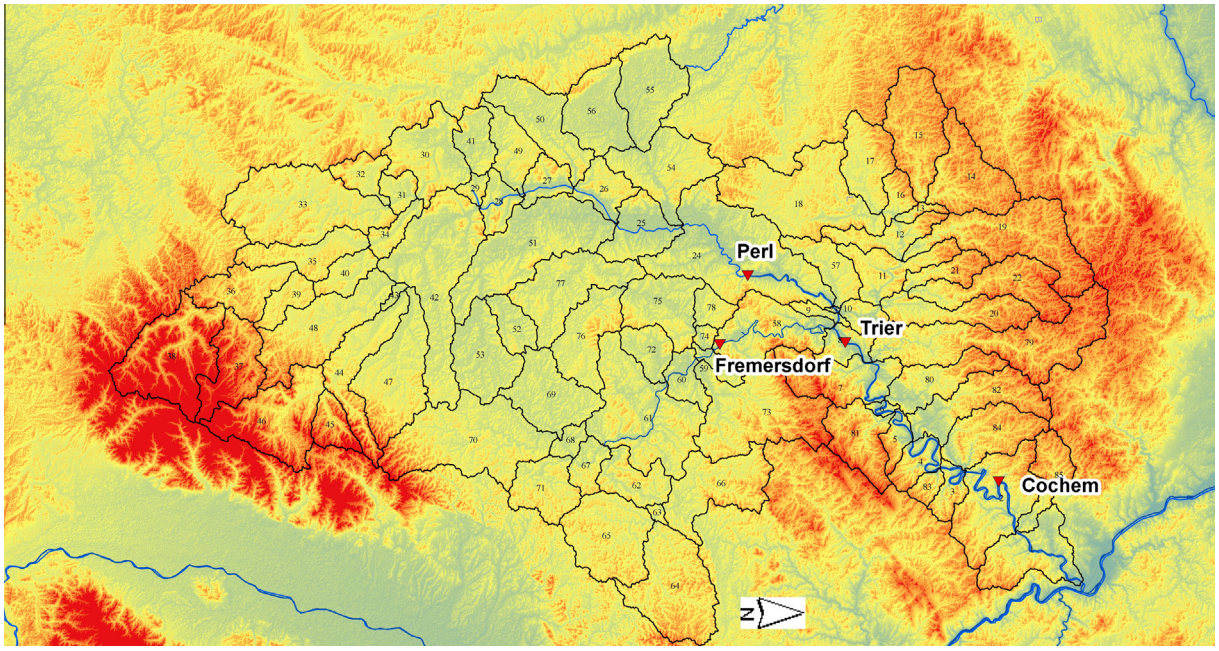

Fig. 1a. The River Mosel basin with observing stations Perl, Fremersdorf, Trier and Koblenz.

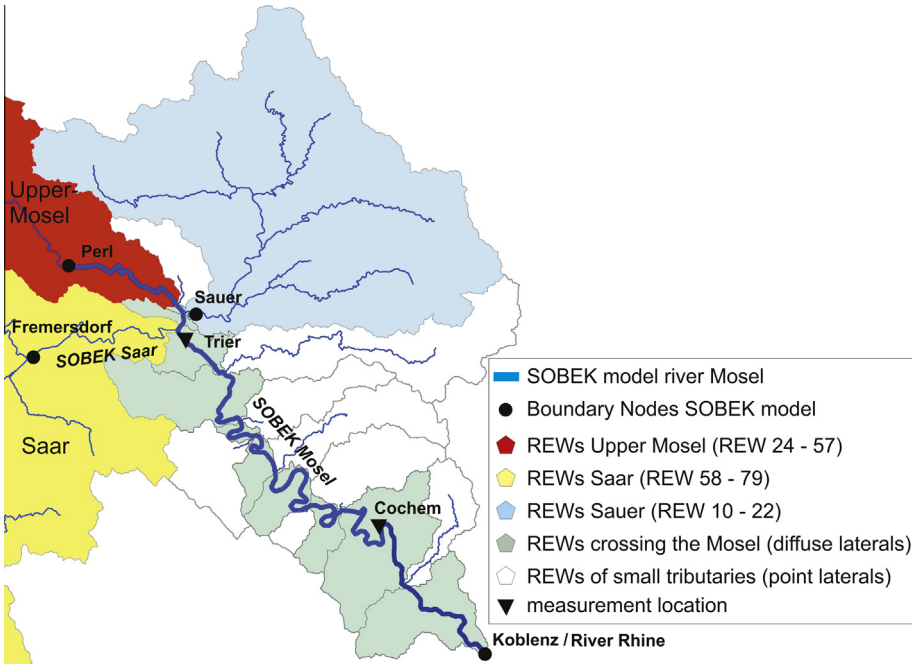

Fig. 1b. Interface between the REW hydrological model and SOBEK in the lower part of the Mosel basin. The boundary nodes of the SOBEK model are indicated with black dots, the gauging stations Trier and Koblenz with back triangles.

boundaries at the nodes Fremersdorf, Perl and Sauer. The inflows are generated by the REW hydrological model. At Koblenz a downstream head boundary condition is imposed, which is given at each time step by the coupled SOBEK model of the River Rhine (a stage-discharge relationship could have been taken instead). The sub-basin outflows of the REW model are added along the modelled river stretch as distributed or concentrated inflows. The MCT is implemented with excactly the same upper boundary conditions and lateral inflows, except the downstream boundary, which is left unconstrained.

6. Results

Next we present the results consisting of a comparison between the original VPM method, referred to as Muskingum–Cunge (MC) solution, and the mass-conservative and steady-stated consistent solution (MCT) presented in this paper. In addition we also report the results for the MC and the MCT solutions, in which we apply the Cappelaere (1997) slope correction. This correction modifies the bed slope in (17) through multiplication by a factor, which depends on the free surface slope. The latter is approximated as the

difference of reach-average water depth over the length of the reach segment. The water depths are estimated from the reach-average discharge through the empirical channel geometry relationships mentioned in Section 5 and reported in more detail in Reggiani et al. (2014). The MC version with the Cappelaere correction is indicated as MCc and the corrected version of the MCT as MCTc. All four solutions are compared against the dynamic wave solution of the SOBEK model, which we denote as Saint–Venant (SV). The time step in the Muskingum method has been selected safely as 1800 s, as longer time steps can potentially lead to a deterioration of the solution. The SOBEK model is set to a time step of 1 h, which can be reduced dynamically during computation if required by the Courant condition. As base case we assign a minimum bed slope of $2.5 \cdot 10^{-4}$, which is imposed as hard minimum value and is in line with the minimum slope assigned in the operational SOBEK model of the Mosel. We note that in the case of the MCc and MCTc solution the slope is reduced, if a correction factor smaller than one is calculated, thus effective slope values smaller than $2.5 \cdot 10^{-4}$ are in this case admissible. For the pure reason of analysing the conservation properties of the MC and MCT methods we have also performed simulations with minimum slopes of $1 \cdot 10^{-4}$ and $0.5 \cdot 10^{-4}$ (and thus lower for the MCc and MCTc with the Cappelaere correction). For such flat channels the flow is chiefly driven by surface gradients as the solution becomes more akin to that of the parabolic equation.

Fig. 2 shows an inter-comparison of all four solutions for a minimum slope of $2.5 \cdot 10^{-4}$ with observations on the same graph at Cochem for a selected triple-peak event which occurred during the 9/12/1999–6/1/2000 period. All Muskingum solutions slightly overestimate the maximum peaks, however the rising as well as falling limbs and the peak timing are well captured and in line with the SV solution. We note that for the selected slope the discharge estimates for MC and MCT are quite similar.

Fig. 3 demonstrates the discrepancy of the storage of the MC approach vs. the storages of the MCT and MCTc solutions. The vertical axis represents the cross section areas at Cochem and Trier over the 9/12/1999–6/1/2000 period. The area is calculated as computed reach storage divided by the uniform reach length of 1 km and acts as proxy for storage. It is evident that the MC formulation with parameters k and ϵ structurally underestimates reach storage and thus reach-average cross-sections by about 34% (slope of $2.5 \cdot 10^{-4}$) with respect to the MCT storage formulation (C.5) based on the corrected parameters k^* and ϵ^*. Column 6 in Table 2 summarizes the overall network storage errors for different slope values.

The effect of the storage error becomes clear if we evaluate the reach-average mean depth from the cross section. This quantity is needed to draw the looped stage-discharge curves depicted in Fig. 4 for the MC and the MCT solutions respectively, which are compared against the curves obtained with the SOBEK model for surveyed sections at Cochem and Trier. We note that the loop is not very pronounced, because the Mosel behaves quasi-kinematic given slopes of $2.5 \cdot 10^{-4}$ and higher. While the empirical cross sections constitute approximations of the actual ones and differences are therefore to be expected, it is clear that the MCT solution reproduces the curves adequately over the entire flow range. The MC solution on the other hand systematically underestimates the reach-average stage, thus exposing the systematic storage estimation error of the MC vs. the MCT. Fig. 5 finally shows for pure demonstration purposes the loops for the (unrealistic) minimum slope of $0.5 \cdot 10^{-4}$ which are clearly more pronounced as one would expect.

Last but not least the reader is reminded that the simulations have been performed over a consecutive period of 6 years, involving multiple peak events. In presence of minimum slopes of $2.5 \cdot 10^{-4}$, both the MC and the MCc loose slightly mass at Cochem with respect to the MCT and MCTc (Column 4 of Table 2). In this context we note that only a minor portion of about 10% of the total network length used in the model (2101 km) has a minimum slope of $2.5 \cdot 10^{-4}$, while the remaining 90% are steeper. The overall mass loss remains therefore quite limited when compared against the total volume transited at Cochem (ca. $67.17 \cdot 10^9$ m^3). This would change however, if the entire network would be flatter. As the slope falls below $2.5 \cdot 10^{-4}$, a situation arises in which the flow is driven essentially by free surface gradients. The mass error for MC and MCc persists, while MCT and MCTc remain fully conservative with a relative error in the order of 1E-16 (Column 5 in Table 2). The relative mass error is evaluated as:

$$\text{rel. mass error } (\%) = \frac{V_0 + \sum_{i=1}^{n} (\bar{I}_i - \bar{O}_i + \bar{Q}_i^L)\Delta T - V_T}{\sum_{i=1}^{n} \bar{O}_i \Delta T} \times 100 \quad (18)$$

where ΔT is the simulation timestep, $T = n \cdot \Delta T$ is the 6-year simulation period, V_0 and V_T are the total initial and final volume stored in the network, $(\bar{I}_i + \bar{Q}_i^L)$ is the total network inflow (lateral inflow and inflow at network head nodes) averaged over the timestep i and $\bar{O}_i$ is the basin outflow at Cochem, also averaged over the timestep.

As a concluding remark we observe that the mass loss for the MC/MCc becomes much more apparent when using a straight channel

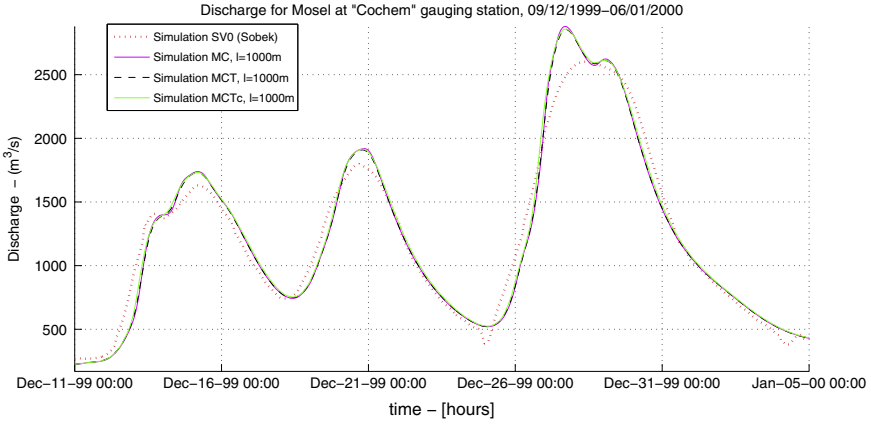

Fig. 2. Discharge values for the 9/12/1999–6/1/2000 event at Cochem for SOBEK, the MC (variable-parameter Muskingum–Cunge) and the MCT/MCTc (Muskingum–Cunge–Todini and Muskingum–Cunge–Todini with Cappellaere correction) solutions. The scope is to show that the errors in representing reality (observed flood wave) using the simplified models together with the approximate cross sections is of the same order of magnitude as the full Saint Venant equations based model developed using measured cross sections. L is the reach segment length of 1000 m.

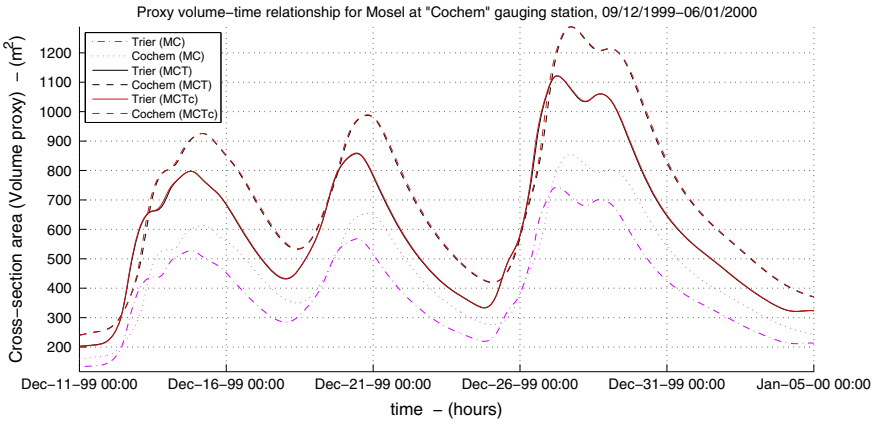

Fig. 3. Reach-average cross section areas for the 9/12/1999–6/1/2000 event at Cochem for SOBEK, the MC (variable-parameter Muskingum–Cunge) and the MCT (Muskingum–Cunge–Todini) solutions (Todini, 2007). The cross section areas serve as proxy for the reach storage. The interest in this figure is focused on comparing the MC against the MCT.

Table 2
Mass balance analysis, Cochem, 1996–2001.

Case	Characteristics	Min. slope	Cum. outflow (mm)	Rel. mass error (%) Eq. (18)	Mass error (%) Eq. (13) and (C.5)
Observed	Measured discharge	N/A	2.33*E*+03	N/A	N/A
SV	726 Nodes, $\Delta t = 1hr$	$2.5 \cdot 10^{-4}$	2.40250*E*+03	1*E*−16	N/A
MC	$\Delta x = 1$ km,$\Delta t = 1800$ s	$2.5 \cdot 10^{-4}$	2.40052*E*+3	0.087	33.83
		$1.0 \cdot 10^{-4}$	2.40061*E*+3	0.082	33.97
		$0.5 \cdot 10^{-4}$	2.40070*E*+3	0.077	33.81
MCc	$\Delta x = 1$ km,$\Delta t = 1800$ s	$2.5 \cdot 10^{-4}$	2.40051*E*+3	0.088	33.82
		$1.0 \cdot 10^{-4}$	2.40050*E*+3	0.088	33.66
		$0.5 \cdot 10^{-4}$	2.40031*E*+3	0.097	33.81
MCT	$\Delta x = 1$ km , $\Delta t = 1800$ s	$2.5 \cdot 10^{-4}$	2.40254*E*+3	1*E*−17	0.00
		$1.0 \cdot 10^{-4}$	2.40253*E*+3	1*E*−16	0.00
		$0.5 \cdot 10^{-4}$	2.40252*E*+3	1*E*−16	0.00
MCTc	$\Delta x = 1$ km , $\Delta t = 1800$ s	$2.5 \cdot 10^{-4}$	2.40254*E*+3	1*E*−16	0.00
		$1.0 \cdot 10^{-4}$	2.40252*E*+3	1*E*−16	0.00
		$0.5 \cdot 10^{-4}$	2.40251*E*+3	1*E*−15	0.00

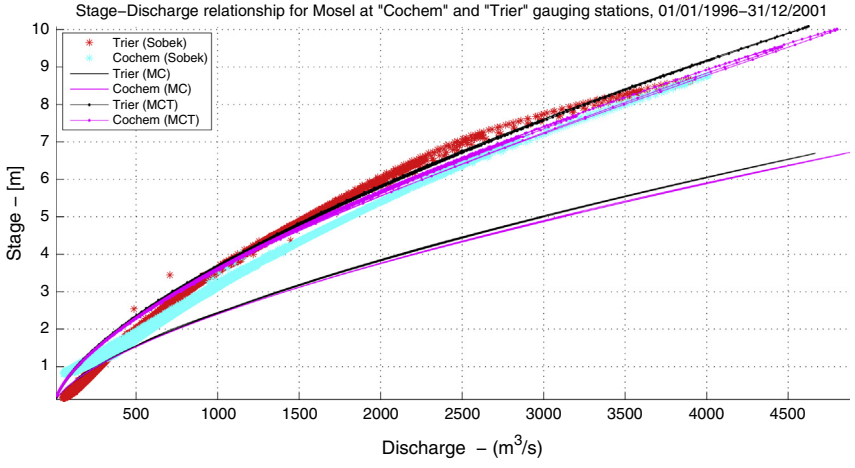

Fig. 4. Looped stage-discharge curves at Cochem and Trier for SOBEK, the MC (variable-parameter Muskingum–Cunge) and the MCT (Muskingum–Cunge–Todini) solutions, minimum slope $2.5 \cdot 10^{-4}$.

with inflow concentrated at the upper end. In a natural dendritic system such as the Mosel, where (*a*) the inflow is distributed more or less uniformly and (*b*) the slope is in the order of 10^{-3} for a large part of the network, the loss is more obfuscated, but is nevertheless present on the theoretical grounds explained in this paper.

7. Discussion

In this final section we would like to discuss the historical perception of the VPM approach from a philosophical and conceptual perspective. Although the Muskingum solution (16), after

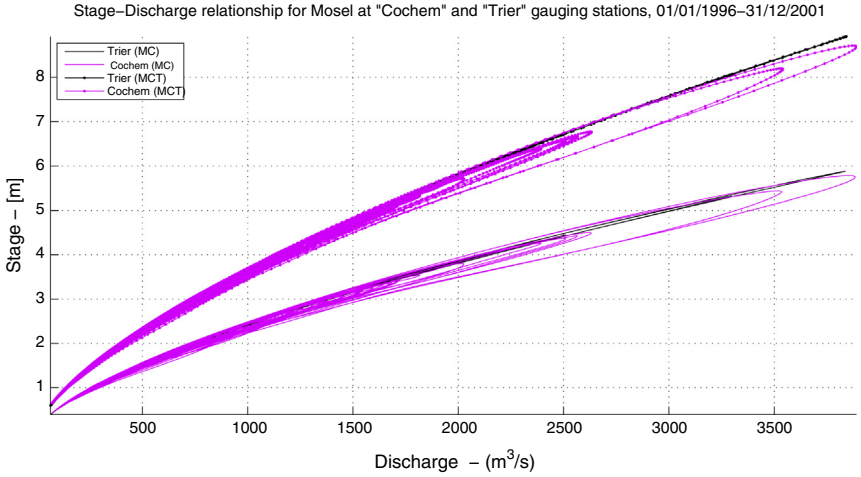

Fig. 5. Looped stage-discharge curves at Cochem and Trier for the MC (variable-parameter Muskingum–Cunge) and the MCT (Muskingum–Cunge–Todini) solutions, minimum slope $0.5 \cdot 10^{-4}$.

integration of the mass balance equation in time, corresponds to the solution of an ordinary differential equation (ODE), in the literature (16) is frequently considered as the solution of a partial differential equation (PDE). Cunge (1969) was the first to draw the parallel between (16) and a time-centred four-point finite difference form of (7) with $D = 0$, with the aim to find a physical interpretation for the variable parameters. From there onwards the tradition of envisaging the VPM method as a discrete form of the DW model persisted (Ponce and Chaganti, 1994; Perumal, 1992; Tang et al., 1999; Wang et al., 2006). By setting the two concepts equal, two things are principally confused: (a) the infinitesimal-scale representation of the mass and momentum conservation as in Eqs. (4) and (5), and (b) the finite-dimension formulation (10) used by McCarthy (1940) as basis of the Muskingum method. The details are discussed hereunder:

- Any finite difference discretization of (7) used as a approximation of (16), is an infinitesimal-scale formulation (infinitesimal along the channel axis and finite over the cross section) which is "stretched" to the finite length of the reach instead of using an equation resulting from its integration over a finite domain. Due to the non-linearity of the equations, the two solutions are different unless the domain is characterised by constant values of the parameters and the flow, as in a channel under uniform flow conditions, a situation which is unlikely to be encountered in natural rivers.
- The finite difference discretized equation for the reach is expressed in terms of water depth and flux gradients, which are *both* evaluated at the reach interfaces. This is a condition which does numerically not guarantee mass balance, as pointed out by Patankar (1980) and acknowledged by several authors (Stelling and Duinmeijer, 2003) and which led to the staggered grid methods chiefly used in two dimensional problems.
- As shown analytically by Gąsiorowski and Szymkiewicz (2007), Eq. (7) does not simultaneously conserve mass and momentum as it is written in a non-divergent form. Consequently any finite difference solution of (7) cannot be conservative either.
- Eq. (16) constitutes a discrete form of an ordinary differential equation (ODE), which results from the finite-scale balance law (10) formulated directly at the reach scale. The mass exchange across the boundary is expressed as inflow/outflow fluxes, which are defined at the reach segment interfaces, while quantities such as reference discharge q, stage y or cross section area A are expressed as reach-averages.
- By solving for mass fluxes on the interface and calculating remaining quantities at the reach midpoint, the VPM method in the conservative form (MCT) presented by Todini (2007) is equivalent to a staggered-grid scheme, in which fluxes are calculated on the boundary of the computational cell and scalar variables at the cell centre. The advantage of using staggered grids in the interest of an accurate numerical solution has been explained by Patankar (1980) and is manifested in case of fluctuating fields or sharp spatial changes of hydrodynamic properties such as roughness.
- The MCT is mass-conservative because the underlying finite-dimension mass balance is written in conservative form (see Appendices A and B) and the flux closure has been corrected for the time-derivative of the parameter product $k \cdot \epsilon$, as shown in Section 3. It is also consistent with the steady state, as the Cunge (1969) parameter k, a reach transition time defined as ratio of cell size and wave speed (Section 3), has been replaced by k^*, the ratio of cell size over velocity. This is a natural consequence of the finite-dimension formulation, as opposed to the analogy drawn with the infinitesimal-scale DW by Cunge; the concept of celerity is implicit in the DW Eq. (7) and the infinitesimal-scale formulation, but extraneous to the finite-dimension conservation law (10). In the case of a wide rectangular channel $c \approx 5/3\ v$ (Henderson, 1966), which highlights the difference in magnitude between the two parameters and the respectively induced error.
- The difference between the Price (2009) finite difference approximation of the DW and the Todini (2007) parameters consists in the fact that the former calculates Q as well as q, A and y as solution of a space–time discretized partial differential equation (PDE) all at the interfaces of a predefined computational grid, while the latter calculates Q on the reach segment interfaces and y and A at the mid-point as solution of a non-linear ordinary differential equation (ODE) for a finite volume.
- While the VPM has been often considered in the hydraulic literature as an approximate routing method suitable for hydrological application, the MCT has been shown to be consistent with mass and momentum conservation. When the diffusive approximation holds, the MCT version of the VPM is thus equivalent to the solution of the dynamic wave equation, but easily

applicable in ungauged basins, where channel geometry information is scarce or unavailable.

8. Summary and conclusions

The paper discusses the corrected VPM method in the mass-conservative and steady-state consistent version (MCT) introduced by Todini (2007) from a novel perspective. The method is cast into the form of a finite-dimension formulation. The principal points of the analysis can be summarised as follows:

- The paper proves that, on the basis of a finite-dimension formulation, the MCT is indeed mass and momentum conservative on theoretical grounds. This is in contrast to the non-linear diffusive wave (DW) equation, which has been shown not to be mass and momentum conservative by Gąsiorowski and Szymkiewicz (2007).
- The finite-difference discretisation of the non-linear DW wave model is generally used to derive the parameters of the VPM method by direct comparison and interpretation. Due to the non-conservative form of the non-linear DW model, these derived VPM formulations are inherently non-conservative, as also repeatedly confirmed in the literature (Cunge, 2001).
- The MCT is based on a finite-dimension mass conservation equation, for which boundary fluxes are closed by non-linear storage-flux relationships. The mass fluxes are evaluated at the segment interfaces (upstream and downstream boundaries) in line with the finite-dimension formulation, while scalar quantities such as the reference discharge, cross-section area and stage are averages evaluated at the reach centre as for staggered-grid solutions.
- The paper is concluded with a real application of a six-year continuous flow simulation for the river Mosel. The VPM method in its original form (Cunge, 1969) is compared against the MCT (Todini, 2007) and the results of the dynamic wave solver SOBEK (Stelling and Duinmeijer, 2003).
- While flood routing is performed satisfactorily by all methods, the looped stage-discharge relationships and the area-time plots clearly show the non-conservative behaviour of the original VPM method in terms of systematic underestimation of the stage. Because the stage is a crucial parameter in evaluating flood risk during forecasting operations, only the mass corrected and steady-state-consistent MCT method can be reliably used for this purpose.

Acknowledgements

We acknowledge the E-OBS dataset from the EU-FP6 project ENSEMBLES and the data providers in the ECA&D project. We also acknowledge the International Commission for the River Rhine (CHR) for providing the digital terrain model for the River Mosel basin.

Appendix A. Proof

The proof for the conservative form of the finite-dimension (11) is provided as follows. The expansion of Eq. (11) under assumption of constant mass density yields the form:

$$\frac{d}{dt}\int_V \mathbf{v}dV + \int_{A_{ex}+A_{in}} \mathbf{n}\cdot\mathbf{v}\mathbf{v}dA - \int_{A_w} \mathbf{n}\cdot\frac{\boldsymbol{\tau}}{\rho}dA + \int_{A_{ex}+A_{in}+A_w} \mathbf{n}\frac{p}{\rho} dA = \int_V \mathbf{g}dV \tag{A.1}$$

where the outer boundary surface A in Eq. (11) has been taken as the sum $A = A_{ex} + A_{in} + A_w + A_{wa}$. In this sum A_{ex} is the downstream reach exit cross section and A_{in} the upstream inflow section; A_w is the wetted channel bed surface, which can be expressed as the product $A_w = P_w \cdot \Delta x$, with P_w the reach-average wetted perimeter and Δx the reach length; finally A_{wa} is the water–air interface at the reach free surface. We note that in (A.1) it is implicitly assumed that only the pressure and kinetic term act normally on the vertical cross sections, while only the shear stresses act tangentially on the bed surface. All other momentum exchanges, such as those acting across the water–air interface A_{wa}, shear stresses acting tangentially to the cross sections, or kinetic terms acting normally to the bed surface, are reasonably neglected. After projection along the channel axis, the vector equation is restated in scalar form:

$$\frac{d}{dt}\left(v\overline{A}\right) + \frac{1}{\Delta x}\left[A_{in}\left(\alpha\overline{v}^2 + \frac{p}{\rho}\right)_{in} - A_{ex}\left(\alpha\overline{v}^2 + \frac{p}{\rho}\right)_{ex}\right] - \frac{P_w}{\rho}\tau_b = gS_0\overline{A} \tag{A.2}$$

with $\overline{A}$ the reach-average cross section, $\overline{v}$ the (scalar) average velocity over the respective inflow or exit cross section and α the Boussinesq coefficient. As common in open channel flow, the shear stress τ_b acting on the bed surface is expressed as a square function of the reach-average velocity v:

$$\tau_b = \frac{\rho g \overline{y} n^2\ v^2}{\overline{R}_H^{4/3}} \tag{A.3}$$

with $\overline{R}_H = \overline{A}/P_w$ the reach-average hydraulic radius and $\overline{y}$ the reach-average water depth in the channel. For uniform flow the difference between square brackets is zero; under steady uniform conditions, (A.2) collapses to Mannings formula. In the non-uniform flow case it is easy to show that no additional non-zero diffusive terms are needed to balance (A.1) and therefore the finite-scale momentum formulation for a reach is fully conservative.

Appendix B. Proof

A mathematical proof that the variable parameter DW equation in the form proposed by Cappelaere (1997) is non-conservative is obtained by transforming the infinitesimal-scale parabolic Eq. (7) into a finite-dimension one through integration over a reach segment of length L (Gąsiorowski and Szymkiewicz, 2007):

$$\frac{\partial}{\partial t}\int_L Q dx + \int_L C\frac{\partial Q}{\partial x}dx + \int_L D\frac{\partial^2 Q}{\partial x^2}dx = 0 \tag{B.1}$$

By exploiting the chain rule of differentiation (B.1) can be restated:

$$\frac{\partial}{\partial t}\int_L Q dx + \int_L \frac{\partial (C\,Q)}{\partial x}dx + \int_L \frac{\partial}{\partial x}\left(D\frac{\partial Q}{\partial x}\right)dx = \int_L \left[Q\frac{\partial C}{\partial x} + \frac{\partial Q}{\partial x}\frac{\partial D}{\partial x}\right]dx \tag{B.2}$$

Thanks to Gauss's theorem the second and third term are converted respectively into convective and diffuse fluxes across the cross-section area A at the reaches ends:

$$\frac{\partial}{\partial t}\int_L Q dx + \left[C\,Q + D\frac{\partial Q}{\partial x}\right]_A = \int_L \left[Q\frac{\partial C}{\partial x} + \frac{\partial Q}{\partial x}\frac{\partial D}{\partial x}\right]dx \tag{B.3}$$

For a linear DW C and D are constants and the r.h.s term is zero, yielding a finite-scale balance law for Q. For variable C and D the integral yields a non-zero residual:

$$R = -\int_L \left[Q\frac{\partial C}{\partial x} + \frac{\partial Q}{\partial x}\frac{\partial D}{\partial x}\right]dx \neq 0 \tag{B.4}$$

proving that the non-linear version of (7) is non-conservative because it cannot be cast into a divergent form. For instance, in

the case of a wide rectangular channel of width B (i.e. $B \gg y$) and an energy line which is parallel to the channel bed (i.e. $\partial y/\partial x \approx 0$), $C(Q)$ becomes the kinematic wave velocity, thus C and D can be expressed as functions of Q only (Chow, 1968):

$$C = 1/\left(m\,\alpha\,Q^{m-1}\right); \qquad D = Q/(2BS_0) \tag{B.5}$$

where

$$\alpha = \left(n\,P_w^{2/3}S_0^{-1/2}\right)^m \tag{B.6}$$

with $m = 3/5$, P_w the wetted perimeter and n the Manning roughness. It is easy to show that (B.4) is always non-zero for non-zero Q and $\partial Q/\partial x$. By equivalence the DW equation as reported by Cappelaere (1997) is not conservative either.

Appendix C. MCT parameters

The mass-conservative and steady-state consistent VPM method presented by Todini (2007) extended to include lateral inflow Q^L $[L^3/T]$ is recapitulated. The outflow $O_{t+\Delta t}$ from a reach segment of length the reach of length Δx is given by a linear combination of variable coefficients and the inflow and outflow at time t and $t+\Delta t$:

$$O_{t+\Delta t} = C_1\,I_{t+\Delta t} + C_2\,I_t + C_3\,O_t + C_4\,\overline{Q^L} \tag{C.1}$$

with $\overline{Q^L} = \frac{1}{2}\left(Q^L_{t+\Delta t} - Q^L_t\right)$. The coefficients expressed in terms of corrected Courant C^* and Reynolds D^* numbers are given by the following expressions:

$$\begin{aligned} C1 &= \frac{-1 + C^*_{t+\Delta t} + D^*_{t+\Delta t}}{1 + C^*_{t+\Delta t} + D^*_{t+\Delta t}} \\ C2 &= \frac{1 + C^*_t - D^*_t}{1 + C^*_{t+\Delta t} + D^*_{t+\Delta t}} \cdot \frac{C^*_{t+\Delta t}}{C^*_t} \\ C3 &= \frac{1 - C^*_t + D^*_t}{1 + C^*_{t+\Delta t} + D^*_{t+\Delta t}} \cdot \frac{C^*_{t+\Delta t}}{C^*_t} \\ C4 &= \frac{2C^*_{t+\Delta t}}{1 + C^*_{t+\Delta t} + D^*_{t+\Delta t}} \end{aligned} \tag{C.2}$$

with

$$C^*_t = \frac{c_t}{\beta_t}\cdot\frac{\Delta t}{\Delta x}; \quad C^*_{t+\Delta t} = \frac{c_{t+\Delta t}}{\beta_{t+\Delta t}}\cdot\frac{\Delta t}{\Delta x} \tag{C.3}$$

$$D^*_t = \frac{q_t}{\beta_t B S_0 c_t \Delta x}; \quad D^*_{t+\Delta t} = \frac{q_{t+\Delta t}}{\beta_{t+\Delta t} B S_0 c_{t+\Delta t}\Delta x} \tag{C.4}$$

where c is the wave celerity and $\beta = \overline{A}\,c/q$ a dimensionless correcting factor with $\overline{A}$ the reach-average cross sectional area calculated from the reach storage V as $\overline{A} = V/\Delta x$. From the shape of the cross section the reach-average stage can be evaluated as $y = y(\overline{A})$. The quantity q is the reach reference discharge, which is approximated using an iterative procedure with two or three support points. All quantities must be evaluated at times t and $t+\Delta t$, respectively. The corrected mass-conservative expression for the reach segment storage is:

$$V_{t+\Delta t} = \frac{(1 - D^*_{t+\Delta t})\Delta t}{2C^*_{t+\Delta t}}\,I_{t+\Delta t} + \frac{(1 + D^*_{t+\Delta t})\Delta t}{2C^*_{t+\Delta t}}\,O_{t+\Delta t} \tag{C.5}$$

References

Cappelaere, B., 1997. Accurate diffusive wave routing. J. Hydraulic Eng., ASCE 123 (3), 174–181.

Chow, V.T., 1968. Handbook of Hydrology. MCGraw Hill, New York, NY.

Cunge, J.A., 1969. On the subject of a flood propagation computation method (Muskingum Method). J. Hydr. Res. 7 (2), 205–230.

Cunge, J.A., 2001. Volume conservation in variable parameter Muskingum–Cunge method – discussion. J. Hydraulic Eng., ASCE 127 (3), 239.

Dooge, J.C.I., 1973. Linear Theory of Hydrologic Systems, USDA Tech. Bull 1468, U.S. Department of Agriculture, Washington DC.

Eringen, A.C., 1980. Mechanics of Continua. R.E. Krieger Pub. Co.

Gąsiorowski, D., Szymkiewicz, R., 2007. Mass and momentum conservation in the simplified flood routing models. J. Hydrol. 346, 51–58.

Hayami, S., 1951. On the Propagation of Flood Waves, Bulletin No 1. Disaster Prevention Research Institute, Kyoto University, Japan.

Henderson, F.M., 1966. Open Channel Flow. Macmillan, New York, NY.

HEC-1: Flood hydrograph package-User's manual, Version 4 (1990), U.S. Army Corps of Engineers, Hydrologic Engineering Center, Davis, CA.

Leopold, L.B., Maddock Jr., T., 1953. The Hydraulic Geometry of Stream Channels and some Physiographic Implications, U.S. Geological Survey Professional Paper 252, 56 pp.

Lighthill, M.J., Whitham, G.B., 1955. On kinematic waves, I Flood movement in long rivers. Proc. Roy. Soc. Lon., 229A.

Liu, Z., Todini, E., 2004. Assessing the TOPKAPI nonlinear reservoir cascade approximation by means of a characteristic lines solution. Hydrol. Processes 19 (10), 1983–2006.

McCarthy, G.T., 1940. Flood Routing, Chap. V Flood Control, The Engineer School, Fort Belvoir, Virginia, pp. 127–147.

Moramarco, T., Pandolfo, C., Singh, V.P., 2008. Accuracy of kinematic wave and diffusion wave approximations for flood routing. 1. Steady analysis. J. Hydrol. Eng. 13 (11), 1078–1088.

Moussa, R., Bocquillon, C., 1996. Criteria for the choice of flood routing methods in natural channels. J. Hydrol. 186, 1–30.

Nash, J.E., 1957. The form of the instantaneous unit hydrograph. IUGG General Assembly of Toronto, vol. III. IAHS Publ.

Ostrowski, M., 1992. A universal module for the simulation of hydrological processes. Wasser und Boden (11), 755–760 (in German).

Patankar, S.V., 1980. Numerical Heat Transfer and Fluid Flow, Hemisphere Publishing Corporation, New York, 197 pp.

Perumal, M., 1992. Hydrodynamic derivation of a variable parameter Muskingum method. Hydrol. Sci J. 39 (5), 431–442.

Ponce, V.M., Yevjevich, V., 1978. Muskingum–Cunge method with variable parameters. J. Hydraulic Division, ASCE 104 (12), 1663–1667.

Ponce, V.M., 1986. Diffusion wave modeling of catchment dynamics. J. Hydr. Eng. 112 (8), 716–727.

Ponce, V.M., Chaganti, P.V., 1994. VPM-Cunge revisited. J. Hydrol 162 (3–4), 433–439.

Ponce, V.M., Lugo, A., 2001. Modelling looped ratings in Muskingum–Cunge routing. J. Hydrol. Eng., ASCE 6 (2), 119–124.

Price, R.K., 1985. Chapter 4: flood routing in rivers, developments in hydraulic engineering. In: Novak, P. (Ed.). Elsevier Applied Science Publishers, London, pp. 129–174.

Price, R.K., 2009. Volume-conservative nonlinear flood routing. J. Hydraul. Eng. 135 (10), 838–845, doi: 10.1061/(ASCE)HY.1943-7900.0000088.

O' Donnell, T., 1985. A direct three-parameter Muskingum procedure incorporating lateral inflow. Hydrol. Sci J. 30 (4), 479–496.

Reggiani, P., Rientjes, T.H.M., 2005. Internal flux parameterisation in the Representative Elementary Watershed (REW) approach: application to a natural basin. Water Resour. Res. 41, W04013. http://dx.doi.org/10.1029/2004WR003693.

Reggiani, P., Rientjes, T.H.M., 2010. Closing horizontal groundwater fluxes with pipe network analysis: an application of the REW approach to an aquifer. Env. Modell. Software. http://dx.doi.org/10.1016/j.envsoft.2010.04.019.

Reggiani, P., Todini, E., Meißner, D., 2014. Analytical solution of a kinematic wave approximation for channel routing. Hydrol. Res. 45 (1), 43–57. http://dx.doi.org/10.2166/nh.2013.157.

Snell, J.D., Sivapalan, M., 1995. Application of the meta-channel concept: construction of the meta-channel hydraulic geometry for a natural channel. Hydrol. Proc. 9, 485–495.

Stelling, G.S., Duinmeijer, S.P.A., 2003. A staggered conservative scheme for every Froude number in rapidly varied shallow water flows. Int. J. Numer. Meth. Fluids 43, 1329–1354.

Stelling, G.S., Verwey, A., 2005. Numerical flood simulation. In: Encyclopedia of Hydrological Sciences. John Wiley & Sons Ltd.

Tang, X., Knight, D.W., Samuels, P.G., 1999. Volume conservation in the variable parameter Muskingum–Cunge method. J. Hydraulic Eng. (ASCE) 125 (6), 610–620.

Todini, E., 2007. A mass conservative and water storage consistent variable parameter Muskingum–Cunge approach. Hydrol. Earth Syst. Sci. 11, 1645–1659. http://dx.doi.org/10.5194/hess-11-1645-2007.

Todini, E., Bossi, A., 1986. PAB (Parabolic and Backwater) an unconditionally stable flood routing scheme particularly suited for real time forecasting and control. J. Hydraul. Res. 24 (5), 405–424.

Wang, G.T., Yao, Ch., Okoren, C., Chen, S., 2006. 4-Point FDF of Muskingum method based on the St. Venant equations. J. Hydrol. 324, 339–349.